



	Experiment title: Mechanical properties of single Au and Fe nano-crystals studied by <i>in situ</i> nano-indentation tests in combination with coherent Bragg diffraction imaging	Experiment number: MA-2841
Beamline: ID01	Date of experiment: Jul 13 th to 16 th , 2016 and Feb 17 th to 21 th , 2017	Date of report: 7 March 2018
Shifts: 9+12	Local contact(s): Steven Leake, 2016 and Tobias Schüllli, 2017	<i>Received at ESRF:</i>

Names and affiliations of applicants (* indicates experimentalists)

E. RABKIN (Technion – Israel Institute of Technology, Haifa 32000, Israel)

G. BEUTIER*, M. VERDIER* (SIMAP, CNRS, Univ. Grenoble Alpes, 38000 Grenoble, France)

T.W. CORNELIUS*, F. LAURAUX*, S. LABAT*, M.-I. RICHARD*, O. THOMAS* (Aix-Marseille Université, Université de Toulon, CNRS, IM2NP, Marseille, France)

Report:

The aim of this experiment was the study of the mechanical properties of FCC Au crystals and BCC Fe crystals by *in situ* nano-indentation in combination with Bragg coherent X-ray diffraction imaging (BCDI). In order to avoid any vibrations induced by moving diffractometer motors we intended to record 3D coherent X-ray diffraction patterns by scanning the energy of the incident X-ray beam instead of rocking the sample. KB mirrors, which are achromatic focusing optics, were mandatory for this experiment. They were delivered by the end of 2016 and commissioned in January 2017- We thus divided our experiment into two parts. During the first part, ordinary Bragg coherent X-ray diffraction patterns were recorded on Au and Fe crystals to select defect free and strain free crystals for the second part which focused on the *in situ* nano-indentation.

Gold and iron crystals were prepared on sapphire substrates by dewetting magnetron sputtered Au, respectively, Fe thin films with a thickness of 45 nm at ~900 °C for at least 24 hours. During the dewetting process the thin films agglomerate forming a large number of well-faceted crystals which are all oriented with the Au(111), respectively, the Fe(110) plane parallel to the substrate surface. For BCDI the 8 keV X-ray beam was focused down to 500 x 500 nm² using a Fresnel zone plate. Bragg coherent X-ray diffraction images of the Fe 110 and the Au 111 Bragg peaks of the corresponding crystals are presented in Fig. 1(a) and (b), respectively. The BCDI of the Au crystal displays well-pronounced size fringes demonstrating its defect free and strain free character. The BCDI of Fe crystals on the contrary only shows thickness fringes while the lateral size fringes are totally blurred because of a large residual strain within the crystals. Due to these experimental findings we decided to perform the nano-indentation experiments on the Au crystals exclusively. The reconstructed phase obtained from the coherent diffraction pattern shown in Fig. 1(c) is presented in Fig. 1(d) demonstrating the successful inversion of a BCDI obtained by scanning the energy.

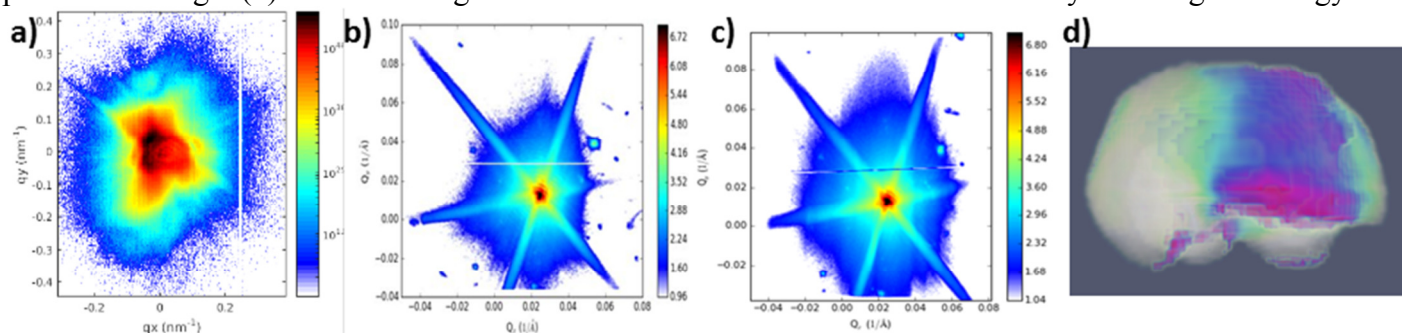


Fig. 1: Integrated Q_x , Q_y slices of the 3D diffraction pattern of a a) rocking curve of a Fe nano-crystal, b) rocking curve of a Au nano-crystal, c) an energy scan of the same Au nano-crystal as in (b). d) 3D reconstructions of the phase from the coherent diffraction pattern shown in (c).

For *in situ* nanoindentation the *in-situ* AFM “SFINX” was installed on the diffractometer. The crystals, the AFM-tip, and the focused X-ray beam were aligned with respect to each other recording AFM-topography (Fig. 2(a)) and scanning X-ray diffraction (Fig. 2(b)) using the k-map approach. Prior to indentation, 3D coherent X-ray diffraction patterns of individual Au crystals were recorded both by ordinary rocking scans and by the energy scanning method. Both techniques provide the same results (Fig. 1(b) and (c)), thus validating the energy scanning approach which was subsequently used for the *in situ* nanoindentation studies. During nano-indentation 2D coherent X-ray diffraction patterns were recorded which were cross-correlated *in situ*. As soon as the AFM-tip touches the upper facet of the Au crystal (indicated by a sharp decrease of the amplitude Fig 2.(c)), the 2D diffraction pattern is modified being clearly visible in the *in situ* cross-correlation (Fig. 2(d)).

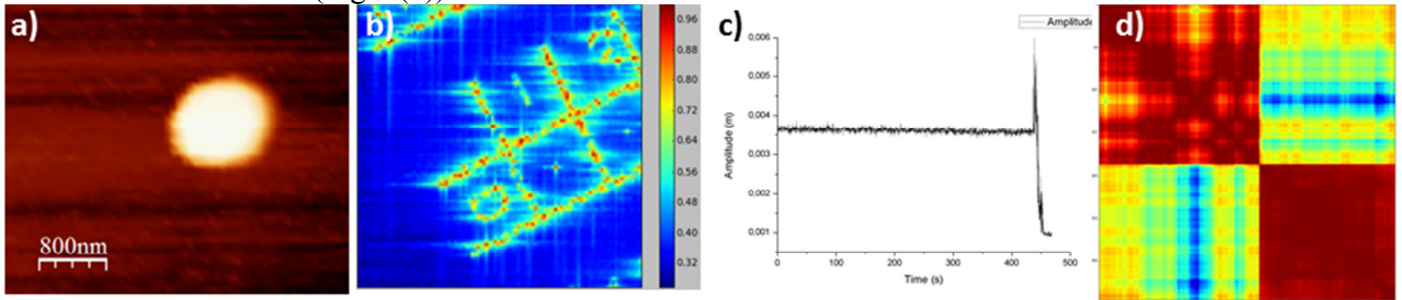


Fig 2: a) AFM topography of a Au nano-crystal and b) K-Map of the patterned Au sample. c) Approach-retract curve of the AFM. d) *In situ* cross-correlation of the 2D diffraction patterns recorded during indentation.

The indentation process was interrupted at pre-defined loads and 3D coherent X-ray diffraction patterns were recorded by scanning the X-ray energy by ± 250 eV. Figure 3(a) to e) display XZ slices of the reconstructed phase of individual Au crystal for : 0 μN , 1.75 μN , 2.75 μN , 4.75 μN and 5.75 μN . We clearly evidence changes in the central part of the diffraction peak itself (Fig. 3(f)), such as a splitting, indicating a modification of the internal strain of the crystal, which translates in the reconstructions by the appearance of a second domain in the crystal. To our knowledge this experiment reported here is the first *in-situ* nano-indentation test combining coherent Bragg diffraction imaging. These experiments are very promising and it paves the way to a better understanding of the onset of plasticity and the different types of defect nucleated in scarce or defect-free nanostructures.

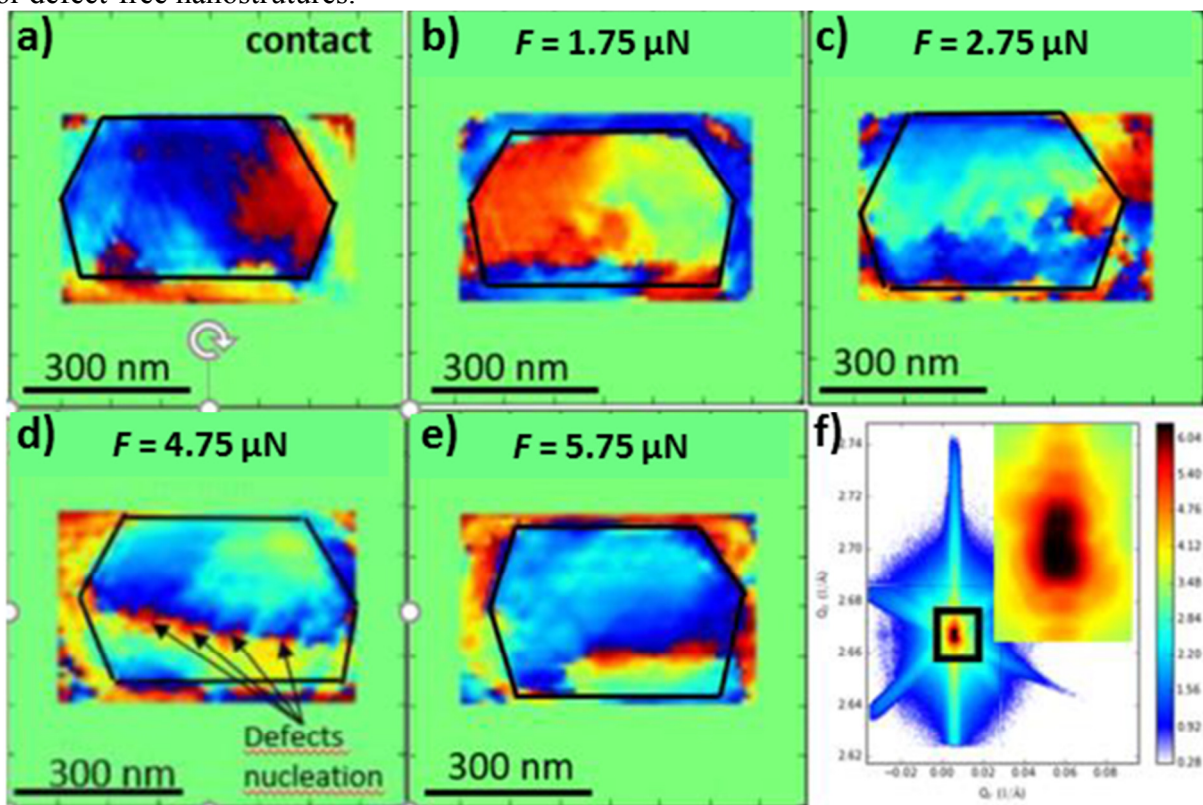


Fig. 3) XZ slices of the reconstructed phase of the same Au crystal under various loads: a) AFM-tip in contact, b) 3rd loading step (1.75 μN), c) 5th loading step (2.75 μN), d) 6th loading step (4.75 μN), e) 8th loading step (5.75 μN). f) Coherent diffraction pattern of the 8th loading step. The inset shows the center of the Bragg peak revealing a splitting.